

# Elemental geochemistry and Nd isotopic characteristics of the metasedimentary rocks from the metamorphic belt in central Jiangxi: Provenance and tectonically environmental constraints\*

HU Gongren (胡恭任)<sup>1,2,3</sup>, LIU Congqiang (刘丛强)<sup>1</sup>, ZHANG Bangtong (章邦桐)<sup>3</sup>  
TANG Hongfeng (唐红峰)<sup>1</sup>, and YU Ruilian (于瑞莲)<sup>2</sup>

<sup>1</sup> Institute of Geochemistry, Chinese Academy of Sciences, Guiyang 550002, China

<sup>2</sup> Department of Environmental Science and Engineering, Huaqiao University, Quanzhou 362021, China

<sup>3</sup> State Key Laboratory for Mineral Deposits Research, Nanjing University, Nanjing 210093, China

**Abstract** The metamorphic belt in central Jiangxi, located in the compound terrain within the Cathaysia, Yangtze Block and Caledonian fold zone of South China, is composed dominantly of meta-argillo-arenaceous rocks, with minor amphibolite. These rocks underwent amphibolite-facies metamorphism. The meta-argillo-arenaceous rocks show large variations in major element composition, but have similar REE patterns and trace element composition, incompatible element and LIE enrichments [high Th/Sc (0.57 – 3.59), La/Sc (1.46 – 12.4), La/Yb (5.84 – 19.0)] and variable Th/U ratios, with  $\Sigma\text{REE} = 129 - 296 \mu\text{g/g}$ ,  $\delta\text{Eu} = 0.51 - 0.86$ , and  $(\text{La}/\text{Yb})_{\text{N}} = 3.95 - 12.9$ . The Nd isotopic model ages  $t_{\text{DM}}$  of these rocks vary from 1597 to 2124 Ma. Their  $^{143}\text{Nd}/^{144}\text{Nd}$  values are low [ $\varepsilon_{\text{Nd}}(0) = -11.4$  to  $-15.8$ ]. Some conclusions have been drawn as follows: (1) The metamorphic rocks in central Jiangxi Province are likely formed in a tectonic environment at the passive continental margin of the Cathaysia massif. (2) The metamorphosed argillo-arenaceous rocks are composed dominantly of upper crustal-source rocks (Al- and K-rich granitic or/and sedimentary rocks of Early Proterozoic), which experienced good sorting, slow deposition and more intense chemical weathering. (3) According to the whole-rock Sm-Nd isochron ages ( $1113 \pm 49$  to  $1199 \pm 26$  Ma) of plagioclase-amphibole (schist) and Nd isotopic model age  $t_{\text{DM}}$  (1597 – 2124 Ma) of meta-argillo-arenaceous rocks, the metamorphic belt in central Jiangxi Province was formed during the Middle Proterozoic (1100 – 1600 Ma).

**Key words** meta-argillo-arenaceous rock; geochemistry; Nd isotope; the metamorphic belt in central Jiangxi Province

## 1 Introduction

Sedimentary rocks bear a great wealth of information about crustal evolution. The compositions of sedimentary rocks have been used to constrain the potential source (e. g. McLennan et al., 1995; Naqvi et al., 1988), to reconstruct the tectonic settings of depositional basins (e. g. Bhatia and Crook, 1986), and to reveal possible paleoclimatic conditions (Nesbitt and Young, 1982). In many cases, particularly in Precambrian domains, sedimentary rocks may be the only preserved record of the ancient crust if the source regions have been covered or destroyed over geological time. Moreover, the geochemistry of sedimentary rocks may help to constrain the average upper crust composition and global crustal evolution models, for example, whe-

ther the average upper crustal composition changed during the Archean-Proterozoic transition (e. g. Gibbs et al., 1986; Condie and Wronkiewicz, 1990a; Taylor and McLennan, 1985, 1995).

In the Le'an-Linchuan-Jinxi-Yingtang region of central Jiangxi, there is a moderately metamorphic rock belt with a length of over one hundred kilometers and a width of 20 kilometers in western Mt. Wuyishan. These metamorphic rocks were metamorphosed and deformed more than one time. There is almost no detailed investigation on the rocks except some research on petrology, mineralogy and Rb-Sr isochronology of metamorphic rocks in the Xiangshan district of central Jiangxi Province (Hu Gongren et al., 1997, 1998a, b, 1999a).

This paper reports the geochemical data of the meta-argillo-arenaceous rocks collected from the metamorphic belt in central Jiangxi Province based on a comprehensive field investigation and lab. analysis. The purpose of the study is to constrain the sources of the sediments, to reveal whether there was any significant Ar-

clean contribution to the sediments or not, and to understand the tectonic settings of the sedimentary basins.

## 2 Geological setting and lithological characteristics

The metamorphic belt in central Jiangxi Province is located in the compound terrain among the Cathaysia, Yangtze Block and Caledonian fold zone of South China [Fig. 1(a)]. These rocks constitute the volcanic basin basement of the Xiangshan and Shengyuan uranium orefields, uranium deposit No. 90. Therefore, studies on the geological evolution and composition of the source region, and the genetic environment of the metamorphic belt in central Jiangxi Province are of important significance in understanding the crustal evolution and uranium mineralization of this area.

The metamorphic belt in central Jiangxi Province, which is composed dominantly of meta-argillo-arenaceous rocks with minor amphibolite, is sporadically distributed throughout northern Xiangshan area, Lixi in the Yihuang area, Maopai in the Linchuan area, and

Maquan in the Yujiang area [Fig. 1(b)]. According to the types, contents, and textures of typical metamorphic minerals, two basic types of meta-argillo-arenaceous rocks have been divided; granulites and schists. Schists are the dominant rock type, which includes sillimanite-mica schist, staurolite-almandite-mica-quartz schist, garnet-mica-quartz schist, hornblende-bearing mica-quartz schist and phyllite schist. The typical mineral assemblage of the schists is quartz + biotite + muscovite, with subordinate garnet  $\pm$  staurolite  $\pm$  K-feldspar  $\pm$  sillimanite  $\pm$  plagioclase  $\pm$  hornblende. Granulites mainly include biotite-plagioclase granulite, mica-plagioclase granulite and mica granulite. The rocks commonly contain mica, up to 70%. Felsic minerals are mainly quartz and plagioclase. They occur mainly in the granulite, with large variations in their proportions of quartz and plagioclase. Amphibolite, moderate- to fine-grained in size, is composed predominantly of hornblende (>80%). It is intercalated locally with fine-grained almandite-mica schist. It occurs mainly as lenses at Guanxia and Makou, northern Xiangshan area, and at Maquan in the Yujiang area.



Fig. 1. (a) Sketch map of tectonic division in central Jiangxi Province. I. Yangtze block; II. Caledonian orogenic zone in South China; III. metamorphic belt in Jiangxi Province; IV. Cathaysia block; V. Mesozoic volcanic rock. ① Guangfeng-Pingxiang deep fault zone; ② Suichuan-Le'an fault zone; ③ Shaowu-Heyuan fault zone; ④ Zhejiang-Fujian-Jiangxi fault zone; ⑤ Lishui-Dapu fault zone. (b) A simplified and distribution map of metamorphic rocks in central Jiangxi Province. 1. Metamorphic rocks in central Jiangxi Province; 2. Neoproterozoic strata; 3. geological boundary; 4. fault; 5. Mesozoic volcanic rock; 6. Caledonian granite; 7. Kalgan red bed; 8. Yangtze block, Shuangqiaoshan Group; 9. sampling site.

## 3 Sampling and analytical methods

Representative samples were collected from the metamorphic belt in Jiangxi Province. Sample localities and sample lithologies are given in Table 1 and shown in Fig. 1(b).

All samples were ground in an agate. The major elements were determined using wet chemical analytical

methods at the State Key Laboratory for Mineral Deposits Research, Nanjing University. The analytical uncertainties are generally better than 5% for most elements. The trace elements were analyzed on a Perkin-Elmer Sciex ELAN 6000 inductively-coupled plasma mass spectrometer (ICP-MS) at the Institute of Geochemistry, Chinese Academy of Sciences. About 50 mg of sample powder was dissolved in Teflon bombs using a HF + HNO<sub>3</sub> mixture. An internal standard solu-

tion containing the single element Rh was used to monitor drift in mass response during counting. The international standards BCR-1 and GSB-3 were chosen to calibrate element concentrations of the measured samples. In-run analytical precision for most elements is less than 3%, whilst reproducibility is generally less

than 5%. Detection limits of the ICP-MS methods for trace elements listed in Tables 2 and 3 are in the range 0.01 – 0.03  $\mu\text{g/g}$  with the following exceptions; Cs (0.158  $\mu\text{g/g}$ ), Rb (0.099  $\mu\text{g/g}$ ) and Sr (0.115  $\mu\text{g/g}$ ). Procedure blanks for all elements were below the detection limits.

**Table 1. Locations and mineral assemblages of the samples from the metamorphic belt in central Jiangxi Province**

Sample No.	Location	Lithology	Qtz	Pl	Ksp	Bt	Ms	Grt	Sil	St	Hb	Chl
Y5	Yihuang	Biotite-plagioclase granulite	A	A	T	A	A	M				
Y61	Yihuang	Biotite-plagioclase granulite	A	A	T	A	A	M				
Y65	Yihuang	Biotite-plagioclase granulite	A	A	T	A	A	M				
Y8	Yihuang	Mica-plagioclase granulite	A	A	T	A	A	M				
X88	Xiangshan	Mica-granulite	A	M	T	A	A	T				
N1-3	Nancheng	Sillimanite-bearing biotite-plagioclase granulite	A	A	T	A	A	M	T			
Y60	Yihuang	Sillimanite-mica schist	M			A	A	T	A			
X97	Xiangshan	Staurolite-almandite-mica-quartz schist	A	T		A	A	M		M		
Y62	Yihuang	Sillimanite-mica schist										
X14	Xiangshan	Staurolite-almandite-mica-quartz schist	A	T		A	A	M		M		
X45	Xiangshan	Staurolite-almandite-mica-quartz schist	A	T		A	A	M		M		
X50	Xiangshan	Garnet-mica-quartz schist	A			A	A	M				
X01	Xiangshan	Garnet-bearing mica schist	A			A	A	T				
X37	Xiangshan	Garnet-mica schist	A	M		M	A	M				T
X47	Xiangshan	Garnet-biotite-quartz schist	A			A	M	M				T
X52	Xiangshan	Garnet-mica-quartz schist	A			A	A	M				T
X67	Xiangshan	Garnet-biotite-quartz schist	A			A	M	M				
X566	Xiangshan	Hornblende-bearing mica-quartz schist	A	M		A	A				T	T
X30	Xiangshan	Biotite schist	M			A	M					
X61	Xiangshan	Biotite schist	M			A	M					
Y9	Yihuang	Garnet-bearing sillimanite-biotite schist	M			A	A	T	A			T
X62	Xiangshan	Mica schist	M			A	A					
X11a	Xiangshan	Garnet-bearing mica schist	A			A	A	T				
X11d	Xiangshan	Garnet-bearing staurolite-mica schist	A			A	A	T				
X51	Xiangshan	Garnet-bearing mica schist	A	M		A	M	T				T
G2	Guanxia	Garnet-mica-quartz schist	A	M		A	A	M				T
G3	Yihuang	Mica-quartz schist	A	M		A	A					T
G4	Yihuang	Hornblende-bearing mica-quartz schist	A	M		M	A			M		T
Zk320	Xiangshan	Phyllite schist	M			A	A					T
Zk47	Xiangshan	Phyllite schist	M			A	A					T

Note: Only major silicate minerals are listed. A (abundant), >20%; M (minor), 5% – 20%; T (trace), <5%. Mineral abbreviations: Qtz. quartz; Pl. plagioclase; Ksp. K-feldspar; Bt. biotite; Ms. muscovite; Grt. garnet; Hb. hornblende; Sil. sillimanite; St. staurolite; Chl. chlorite.

For Rb-Sr isotope analysis, the samples were decomposed in the Teflon bombs using  $\text{HClO}_4 + \text{HF}$  and then separated by the cation exchange technique. The Rb and Sr isotopic analysis of the samples was conducted on a VG-354 mass spectrometer at the Modern Analytical Center of Nanjing University. Numerous analyses yielded a mean value of  $0.71022 \pm 0.00004$  ( $2\sigma$ ) for NBS 987 Sr standard and  $1 \times 10^{-8} - 2 \times 10^{-8}$  g, and  $1 \times 10^{-9} - 2 \times 10^{-9}$  g for the blank value of Rb and Sr, respectively (Li Jieyuan, 1992).

For Sm-Nd isotope analyses, 20 – 50 mg of the whole-rock sample was spiked with appropriate amounts of a mixed  $^{149}\text{Sm}$ - $^{150}\text{Nd}$  spike in the radiogenic isotope laboratory at Beijing Research Institute of Ura-

nium Geology. The spiked samples were digested in Teflon bombs using doubly distilled  $\text{HF-HNO}_3$  at ca 180. Two-stage cation exchange column procedures were used for REE pre-concentration and subsequent Sm-Nd separation. Sm-Nd were loaded with phosphoric acid on Re double filaments. Isotope ratios were determined on a VG354 multicollector mass spectrometer in static mode. Replicate analyses of La Jolla Nd, Ames Nd and Ames Sm standards yielded  $^{143}\text{Nd}/^{144}\text{Nd}$  ratios of  $0.511844 \pm 20$ ,  $0.512117 \pm 14$  and  $^{149}\text{Sm}/^{152}\text{Nd}$  ratio of  $0.516891 \pm 26$ , respectively. Nd isotopic ratios were normalized to  $^{146}\text{Nd}/^{144}\text{Nd} = 0.7219$ , and Sm to  $^{149}\text{Sm}/^{152}\text{Sm} = 0.56081$ .  $\epsilon_{\text{Nd}}$  values were calculated assuming current CHUR  $^{143}\text{Nd}/^{144}\text{Nd} = 0.512638$  and

$^{147}\text{Sm}/^{144}\text{Nd} = 0.1967$ , and the decay constant for  $^{147}\text{Sm} = 6.54 \times 10^{-12} \text{ year}^{-1}$  (Li Jieyuan, 1992; Hu Gongren et al., 1998a).

#### 4 The type and geochemistry of the primary rocks

Major element compositions of 30 samples are

presented in Table 2.

In the K-A diagrams (diagrams omitted; He Gaopin, 1986), all the samples were plotted into the sedimentary rock field. In the Nigli [(al + fm)-(c + alk)]-Si diagrams [Winkler, 1976, Fig. 2(a)], samples were plotted into the argillo-arenaceous rock field. On the ACF (diagrams omitted; Condie et al., 1992) and (Al +  $\Sigma\text{Fe}$  + Ti)-(Ca + Mg) (Wang Ren-

Table 2. Major element compositions (%) of metasediments from the metamorphic belt in central Jiangxi

Number	1	2	3	4	5	6	7	8	9	10	11	12	13	14	15
Sample No.	Y5	Y61	Y65	Y8	X88	N1-3	Y60	X97	Y62	X14	X45	X50	X01	X37	X47
SiO <sub>2</sub>	68.08	67.45	68.92	69.23	68.78	71.36	60.12	60.50	54.86	62.02	68.89	69.44	63.87	59.25	75.30
TiO <sub>2</sub>	0.74	0.18	0.19	0.73	0.83	0.57	0.40	0.37	0.36	0.70	0.68	0.49	0.72	1.16	0.68
Al <sub>2</sub> O <sub>3</sub>	14.35	15.35	12.28	14.25	13.76	12.69	18.10	14.40	17.48	16.75	14.09	13.99	17.97	19.09	10.54
Fe <sub>2</sub> O <sub>3</sub>	0.91	2.50	1.70	2.05	3.98	0.50	2.16	3.71	3.49	3.26	1.90	0.55	2.33	1.83	1.52
FeO	5.13	3.00	4.70	3.02	2.06	5.16	5.54	4.99	7.31	5.94	4.45	4.50	3.96	7.71	4.55
MnO	0.11	0.09	0.07	0.15	0.15	0.15	0.09	0.13	0.36	0.17	0.06	0.19	0.08	0.13	0.10
MgO	2.41	2.30	2.40	2.23	1.59	2.32	3.10	2.90	4.20	3.71	2.51	1.87	2.06	3.68	1.76
CaO	0.83	1.30	0.80	1.19	0.30	1.37	0.80	1.10	2.50	0.44	0.77	2.62	0.40	0.56	0.66
Na <sub>2</sub> O	1.30	3.22	0.97	1.42	3.13	1.30	1.10	1.00	1.92	0.62	1.29	2.96	1.16	0.77	1.47
K <sub>2</sub> O	3.38	2.19	3.79	3.48	2.04	3.07	4.60	3.88	3.79	3.45	2.94	1.83	3.94	4.23	1.77
P <sub>2</sub> O <sub>5</sub>	0.23	0.93	0.80	0.25	0.26	0.23	0.83	0.80	0.80	0.13	0.05	0.87	0.14	0.30	0.06
LOI	1.72	1.40	2.79	1.11	2.35	1.09	3.02	5.61	2.70	2.01	1.40	1.65	2.70	1.01	1.01
Total	99.19	99.91	99.41	99.11	99.23	99.81	99.86	99.39	99.77	99.20	99.91	99.39	99.33	99.72	99.42
CIA	66.40	60.54	63.38	63.27	63.53	61.67	68.73	64.74	59.70	75.05	67.68	54.73	72.54	73.25	65.42
CIW	79.92	66.68	80.13	75.94	70.68	73.53	84.76	79.66	69.30	90.04	80.00	59.31	87.36	89.05	74.19
Number	16	17	18	19	20	21	22	23	24	25	26	27	28	29	30
Sample No.	X52	X67	X566	X30	X61	Y9	X62	X11a	X11d	X51	G2	G3	G4	Zk320	Zk47
SiO <sub>2</sub>	67.58	70.04	76.07	57.94	63.76	57.25	64.89	64.87	63.09	62.02	69.01	61.67	75.11	61.66	54.87
TiO <sub>2</sub>	0.78	0.72	0.57	0.75	0.82	1.16	0.62	0.72	0.66	0.70	0.71	0.73	0.77	0.80	0.87
Al <sub>2</sub> O <sub>3</sub>	15.21	13.52	9.85	16.43	17.13	19.09	17.01	17.87	18.01	16.75	13.55	17.89	10.85	17.70	19.85
Fe <sub>2</sub> O <sub>3</sub>	4.38	0.93	1.57	1.93	1.14	1.83	1.19	2.31	1.01	3.26	1.73	2.05	1.67	3.69	3.98
FeO	1.85	4.25	2.66	5.65	5.66	7.71	6.01	3.98	3.83	5.94	4.59	5.55	2.56	3.04	6.23
MnO	0.03	0.13	0.14	0.20	0.12	0.13	0.11	0.08	0.16	0.17	0.06	0.08	0.15	0.12	0.10
MgO	1.70	1.92	1.22	2.92	2.40	3.68	2.35	2.06	4.99	3.71	1.98	2.61	1.32	2.61	3.50
CaO	0.14	1.83	2.34	2.53	0.12	0.56	0.17	0.40	0.45	0.44	1.78	1.73	2.44	1.73	1.18
Na <sub>2</sub> O	0.21	3.97	2.66	1.18	1.51	0.77	1.50	1.26	0.92	0.62	0.89	1.15	2.56	1.15	1.32
K <sub>2</sub> O	3.68	1.61	0.64	4.52	3.96	4.23	3.95	3.94	3.65	3.45	2.94	3.55	0.94	3.62	4.56
P <sub>2</sub> O <sub>5</sub>	0.19	0.14	0.08	0.15	0.16	0.30	0.15	0.14	0.13	0.13	0.05	0.09	0.08	0.21	0.22
LOI	3.29	0.90	1.30	5.20	2.82	2.41	1.52	1.85	2.52	2.01	1.96	2.00	1.40	3.00	3.02
Total	99.04	99.96	99.10	99.40	99.60	99.12	99.47	99.48	99.42	99.20	99.25	99.10	99.85	99.33	99.70
CIA	76.76	53.61	51.36	58.94	71.16	73.08	70.63	71.69	74.15	75.11	62.83	71.78	53.01	66.59	68.08
CIW	95.94	57.62	53.17	71.52	86.35	88.91	85.65	86.25	88.41	90.14	73.82	84.74	55.91	77.99	82.17

Note: For sample Nos. and lithological characters, see Table 1. CIA = [Al<sub>2</sub>O<sub>3</sub>/(Al<sub>2</sub>O<sub>3</sub> + CaO\* + Na<sub>2</sub>O + K<sub>2</sub>O)] × 100; CIW = [Al<sub>2</sub>O<sub>3</sub>/(Al<sub>2</sub>O<sub>3</sub> + CaO\* + Na<sub>2</sub>O)] × 100 (in molecular proportion).

min, 1987) diagrams [Fig. 2(b)], the samples were plotted into the greywacke, clay rock and shale fields and are distinctive from the volcanic rocks. On the SiO<sub>2</sub>/Al<sub>2</sub>O<sub>3</sub>-(CaO + Na<sub>2</sub>O)/K<sub>2</sub>O (Gromet et al., 1984) diagrams (diagrams omitted), samples were plotted into the argillo-arenaceous sedimentary rock region. In the La/Yb- $\Sigma\text{REE}$  (Reimer et al., 1985) discrimination diagram [Fig. 2(c)], samples were plotted into the sandy and complex sandstone and straddle

the shale and clay rock fields. In the K<sub>2</sub>O-TFe<sub>2</sub>O<sub>3</sub>-Al<sub>2</sub>O<sub>3</sub> diagram of Wronkiewicz and Condie [1989, Fig. 2(d)], these samples were plotted into the fields for NASC (North American Shale Composite) and residual clays, showing that the sources were affected by granite and tonalite. All these go to indicate the original rocks of meta-argillo-arenaceous rocks are mainly the greywacke, clay rock and shale.

#### 4.1 Element geochemical results

As given in Table 2, the major element compositions of meta-argillo-arenaceous rocks vary from 54.87% to 76.07% for SiO<sub>2</sub>, from 9.85% to 19.85% for Al<sub>2</sub>O<sub>3</sub>, from 1.47% to 5.84% for TFe<sub>2</sub>O<sub>3</sub>, from 0.43% to 1.90% for MgO, and from 0.64% to 4.60% for K<sub>2</sub>O (Table 2). The mica-rich and garnet-rich argillaceous rocks have relatively low contents of SiO<sub>2</sub>, CaO, and Na<sub>2</sub>O and relatively high contents of Al<sub>2</sub>O<sub>3</sub>, TFe<sub>2</sub>O<sub>3</sub>, K<sub>2</sub>O and MgO, while the quartz-rich and plagioclase-rich arenaceous rocks have high contents of SiO<sub>2</sub>, CaO and Na<sub>2</sub>O and low contents

of Al<sub>2</sub>O<sub>3</sub>, TFe<sub>2</sub>O<sub>3</sub>, K<sub>2</sub>O and MgO. K<sub>2</sub>O contents in the rocks are associated mainly with the mica-group minerals. The reason why samples X566, G4 and X47 have abnormally high SiO<sub>2</sub> contents and low Al<sub>2</sub>O<sub>3</sub> and K<sub>2</sub>O contents is the presence of abundant quartz but the absence of the mica-group minerals in those samples. The relatively high CaO and Na<sub>2</sub>O contents of samples X50 and G4 are probably due to the presence of plagioclase in them. Obviously, various kinds of rock-forming minerals and their contents constrain the major element compositions of the rocks.

Although obvious variations are noticed in major element composition, the REE patterns and some trace

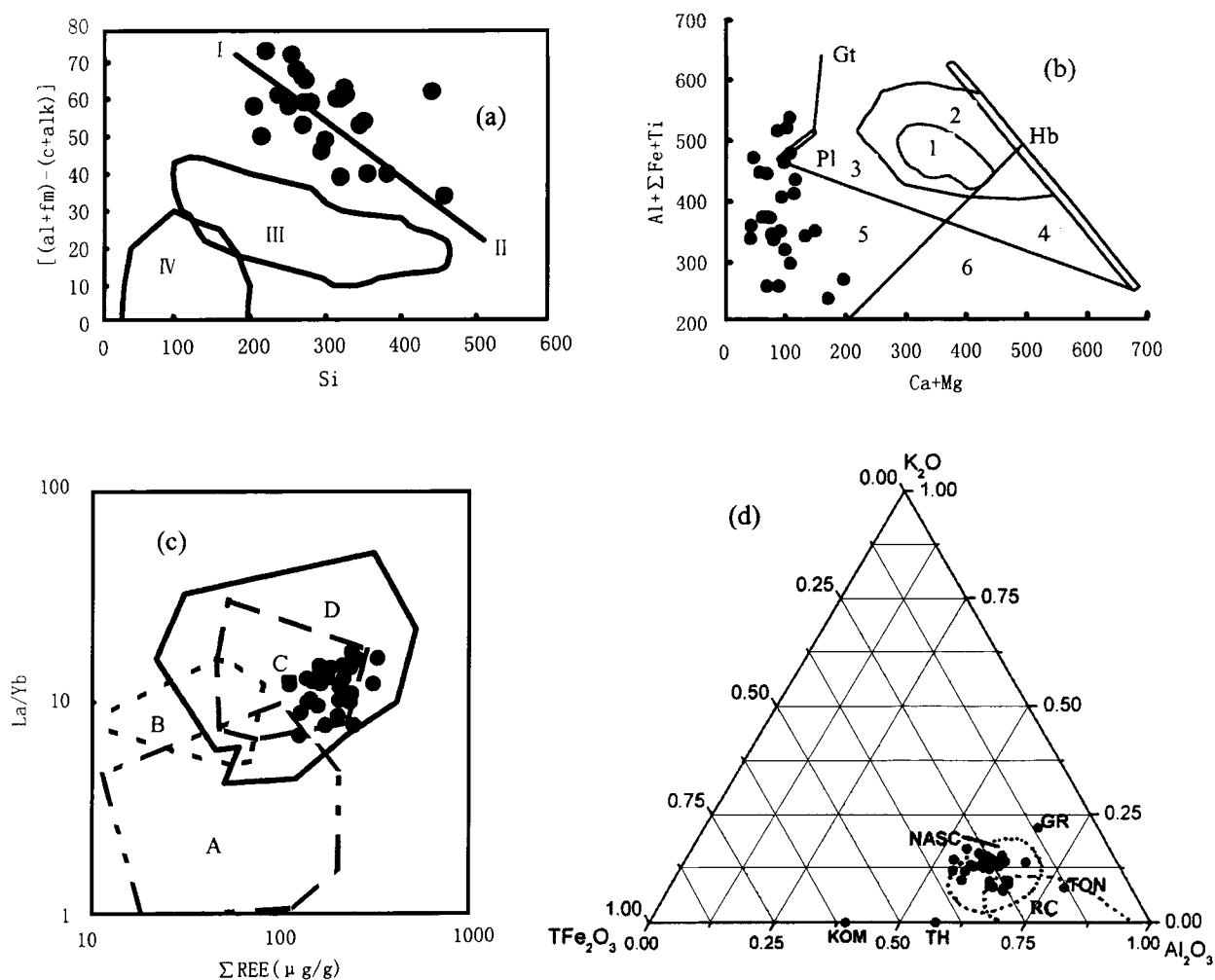


Fig. 2. (a) The (al + fm)-(c + alk)-Si diagram; (b) (Al +  $\Sigma$ Fe + Ti)-(Ca + Mg) diagram; (c) La/Yb- $\Sigma$ REE diagram (Reimer et al., 1985); and (d) K<sub>2</sub>O-TFe<sub>2</sub>O<sub>3</sub>-Al<sub>2</sub>O<sub>3</sub> diagram of meta-argillo-arenaceous rocks from the metamorphic rock belt in central Jiangxi Province (Wronkiewicz and Condie, 1989). I. Argillaceous sediment; II. sandy sediment; III. volcanic rock; IV. calcareous sediment. 1. Basic pyrogenous rock; 2. basic pyrogenous rock and variety; 3. intermediate pyrogenous rock, basic volcanic complex and argillaceous sediment-tuff; 4. carbonatite sediment-tuff; 5. clay, argillaceous rock, arkose and argillo-calcareous malmstone; 6. clay, dolomitic and argillo-calcareous rock. A. Plagioclase-hornblendite; B. carbonatite; C. sandy and complex sandstone; D. shale and clay rock; Hb. hornblende; Gt. garnet; Pl. plagioclase; TON. tonalite; NASC. North American Shale Composite; GR. granite; TH. tholeiite; KOM. komatiite; RC. residual clay.

element contents are very similar (Tables 3 and 4, Figs. 3 and 4). Samples are characterized by the high total REE ( $\Sigma\text{REE} = 129 - 296 \mu\text{g/g}$ ) and high LREE (LREE =  $114 - 256 \mu\text{g/g}$ ) (Table 4). Their REE patterns show moderate negative Eu anomalies ( $\delta\text{Eu} = 0.51 - 0.86$ ), LREE enrichment [ $(\text{La}/\text{Eu})_N = 4.48 - 7.28$ ,  $(\text{La}/\text{Yb})_N = 3.95 - 12.9$ ] and flat HREE pat-

terns [ $(\text{Eu}/\text{Lu})_N = 0.86 - 2.47$ ] (Table 4, Fig. 3).

From the spider diagram of trace elements (Fig. 4), it can be seen that samples are relatively depleted in Sr, Nb, Ti, P and Sc, with a remarkable negative Ba anomaly ( $\delta\text{Ba} = 0.10 - 0.93$ ). The Zr/Y ratios (4 - 8) of samples are similar to those (2 - 7) of the Proterozoic-group shales (Condie, 1993).

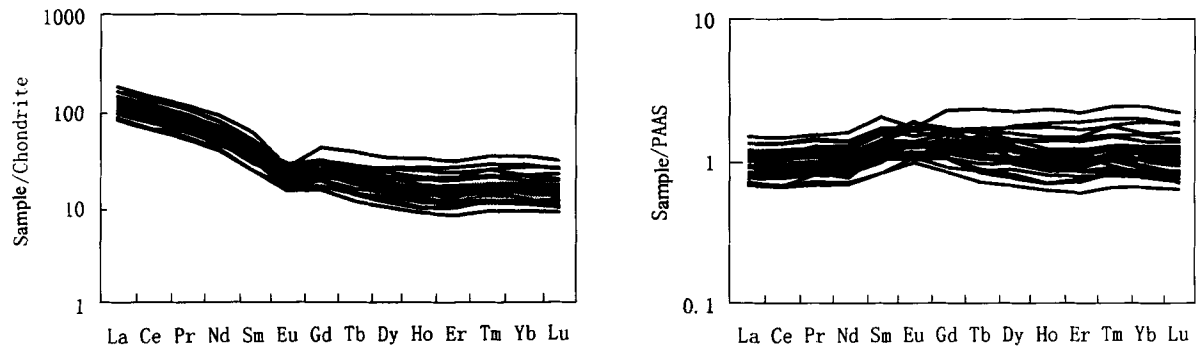


Fig. 3. REE patterns of the meta-argillo-arenaceous rocks from the metamorphic belt in central Jiangxi.

**Table 3.** Trace element concentrations ( $\mu\text{g/g}$ ) of the meta-argillo-arenaceous rocks from the metamorphic belt in central Jiangxi

Number	1	2	3	4	5	6	7	8	9	10	11	12	13	14	15
Sample No.	Y5	Y61	Y65	Y8	X88	N1-3	Y60	X97	Y62	X14	X45	X50	X01	X37	X47
Li	132	52.8	50.6	50.9	45.2	41.2	77.4	103	87.7	25.8	39.4	36.8	34.5	40.0	39.1
Sc	15.1	11.2	13.5	7.31	12.2	10.2	19.2	22.0	25.0	8.81	7.10	7.69	18.7	9.01	8.19
V	139	84.0	89.6	97.3	99.2	97.2	139	119	119	80.0	63.5	64.1	150	90.3	75.9
Cr	114	74.1	98.2	89.6	90.3	89.2	113	94.1	163	49.5	197	135	94.2	70.3	157
Co	37.9	15.2	17.0	28.5	38.6	40.6	23.6	26.7	23.1	8.74	13.8	11.4	18.5	28.8	14.1
Ni	62.2	36.4	38.6	31.9	45.5	47.5	64.7	49.6	65.2	20.1	31.2	22.0	39.4	34.4	72.1
Cu	99.0	23.9	25.9	41.8	55.7	74.9	36.6	66.8	138	45.6	20.1	35.7	11.1	13.9	52.8
Zn	133	97.6	102	77.0	101	114	132	189	169	69.1	73.3	103	153	105	82.7
Ga	23.2	15.4	16.8	14.6	16.5	17.5	24.4	24.3	22.2	17.0	10.3	19.4	28.2	17.8	14.7
Ge	2.26	1.50	1.79	1.28	1.89	2.15	1.79	2.89	3.51	1.61	1.64	2.58	2.49	2.06	2.01
As	2.13	-	55.8	1.82	1.56	2.67	-	-	-	1.81	10.9	3.00	1.78	3.39	4.20
Rb	172	81.4	145	73.1	169	174	166	183	178	69.5	85.6	123	193	114	88.4
Sr	209	210	103	211	98.9	64.9	109	71.7	272	129	144	163	82.6	49.8	35.4
Y	23.7	20.5	27.7	15.6	19.7	18.7	27.1	29.0	58.1	22.6	28.3	25.9	31.7	31.3	22.3
Zr	134	128	191	133	121	111	177	147	314	192	210	118	210	192	180
Nb	16.1	11.8	13.7	11.5	11.9	13.0	17.3	14.3	19.0	10.4	9.89	12.5	15.2	12.1	12.1
Mo	0.55	0.13	0.09	0.24	0.59	0.90	0.35	0.05	0.60	1.05	0.85	0.79	0.16	0.55	0.69
Cd	0.14	0.05	0.09	0.05	0.04	0.07	0.07	0.11	0.20	0.11	0.03	0.06	0.12	0.13	0.02
Sn	3.14	2.60	3.28	1.62	3.56	3.75	3.75	4.67	3.22	3.96	2.15	2.71	4.61	4.37	3.10
Sb	0.11	-	-	0.06	0.15	0.14	-	-	-	0.20	1.46	0.59	0.13	0.17	0.48
Cs	13.8	6.81	14.5	6.41	13.8	15.1	12.3	16.2	13.7	3.94	7.17	11.9	15.5	5.62	7.36
Ba	718	380	715	313	398	340	1122	288	598	826	304	196	556	334	281
Hf	4.26	4.19	6.14	4.25	4.06	3.47	5.71	4.90	10.3	6.57	6.58	4.18	7.36	6.67	6.02
Ta	1.20	0.76	0.90	0.81	0.75	0.90	1.13	1.08	1.55	0.94	0.80	1.18	1.27	1.06	0.95
W	241	0.20	1.64	208	1.59	306	1.91	1.23	0.77	2.19	1.24	2.07	4.16	211	1.41
Pb	54.3	19.9	27.2	23.4	20.6	18.1	24.8	29.0	43.0	70.0	15.4	62.2	44.9	27.7	14.5
Th	13.8	7.03	8.86	8.77	13.3	11.1	11.2	12.5	18.1	15.0	15.2	12.0	13.6	17.4	14.5
U	2.66	1.47	1.99	1.90	2.73	1.73	2.22	2.34	3.70	2.23	2.85	2.92	4.00	3.34	2.95
Th/U	5.19	4.78	4.45	4.62	4.87	6.42	5.05	5.34	4.89	6.73	5.33	4.11	3.40	5.21	4.92
Zr/Y	5.65	6.24	6.90	8.53	6.14	5.94	6.53	5.07	5.40	8.50	7.42	4.56	6.62	6.13	8.07
Cr/Ti	0.015	0.041	0.052	0.012	0.011	0.016	0.028	0.025	0.045	0.007	0.029	0.028	0.013	0.006	0.023
Cr/Th	8.26	10.54	11.08	10.22	6.79	8.04	10.09	7.53	9.01	3.30	12.96	11.25	6.93	4.04	10.83
La/Y	1.86	1.27	1.12	1.76	1.61	1.86	1.49	1.11	0.99	1.92	1.38	1.13	1.62	1.28	1.61
Th/Sc	0.91	0.63	0.66	1.20	1.09	1.09	0.58	0.57	0.72	1.70	2.14	1.56	0.73	1.93	1.77

Table 3. (to be continued)

Number	16	17	18	19	20	21	22	23	24	25	26	27	28	29	30
Sample No.	X52	X67	X566	X30	X61	Y9	X62	X11a	X11d	X51	G2	G3	G4	Zk320	Zk47
Li	41.5	18.3	8.71	3.96	30.1	13.6	22.9	8.08	16.3	27.7	12.0	3.55	8.73	40.9	36.7
Sc	15.7	7.99	5.29	6.82	15.1	7.46	13.8	7.70	5.81	12.1	7.94	7.23	3.12	16.4	21.0
V	158	92.4	58.7	103	108	84.4	99.9	82.9	66.2	81.7	89.3	108	58.0	139	157
Cr	95.7	72.9	45.7	101	179	117	159	154	207	75.9	124	104	90.5	196	209
Co	29.5	15.1	7.91	20.2	27.6	12.4	25.9	15.3	14.7	36.0	13.1	20.7	17.3	23.1	23.1
Ni	38.8	37.0	16.8	43.0	50.9	24.7	47.6	29.2	32.7	26.1	28.7	45.3	32.0	54.5	63.5
Cu	59.4	30.2	51.1	9.34	118	17.6	133	23.9	25.5	62.9	20.6	11.2	9.37	22.9	30.8
Zn	86.4	81.2	114	109	142	79.7	132	80.9	71.4	105	85.1	112	155	108	153
Ga	23.3	15.9	11.5	17.0	22.1	18.5	20.4	17.0	11.4	17.3	20.4	17.6	12.1	23.4	25.9
Ge	1.72	1.66	1.63	1.73	1.97	1.87	1.90	2.16	1.89	3.67	1.84	1.93	2.19	2.00	2.64
As	2.14	2.00	3.00	3.01	2.38	1.61	3.76	3.43	10.7	2.86	1.40	2.73	2.18	5.33	6.49
Rb	102	82.1	38.9	23.5	124	126	117	116	91.9	122	136	24.0	45.8	177	187
Sr	258	312	105	100	67.8	43.6	62.8	51.0	150	231	45.9	104	84.1	176	181
Y	16.7	24.7	29.4	27.2	23.3	25.0	26.7	24.3	29.7	40.3	26.9	28.1	30.0	39.9	17.1
Zr	177	146	128	190	76.3	219	151	193	199	171	232	197	123	198	87.7
Nb	14.8	11.4	9.13	14.3	11.0	11.5	10.7	13.0	9.87	12.1	12.6	14.1	10.9	15.5	14.0
Mo	0.27	0.81	6.78	3.20	2.33	1.21	1.60	0.66	0.93	0.42	0.98	1.31	0.66	2.81	1.48
Cd	0.04	0.07	0.19	0.38	0.06	0.17	0.03	0.03	0.02	0.12	0.38	0.22	0.05	0.14	0.64
Sn	3.22	1.90	2.34	7.17	3.45	7.70	2.38	3.52	2.65	4.36	8.43	7.25	1.89	6.28	6.39
Sb	0.13	0.64	2.55	0.34	0.64	0.24	0.31	0.25	0.45	0.22	0.26	0.35	0.31	1.78	0.63
Cs	9.24	9.07	2.28	1.77	15.1	9.31	14.1	9.75	7.25	12.1	10.7	1.89	4.63	23.9	16.6
Ba	1021	375	151	154	650	444	613	348	323	148	459	162	114	1002	804
Hf	5.78	4.89	4.19	6.83	3.47	7.68	5.05	6.84	6.79	6.64	8.47	7.09	4.35	6.81	3.77
Ta	1.07	0.79	0.75	1.24	0.85	0.93	0.79	1.18	0.86	1.26	1.04	1.23	0.87	1.15	1.06
W	211	0.82	0.94	2.03	2.88	3.54	2.66	2.80	1.33	284	3.94	2.24	3.45	2.83	2.50
Pb	21.5	21.6	133	10.3	18.7	33.8	16.6	28.5	18.1	98.3	36.6	10.9	15.0	16.1	22.2
Th	11.4	9.68	10.9	17.8	12.7	15.6	12.4	15.9	17.0	18.3	16.6	18.5	11.2	13.8	15.9
U	2.45	2.25	2.66	3.39	2.08	3.14	2.18	3.36	3.26	3.80	3.29	3.46	1.76	2.99	2.64
Th/U	4.30	4.10	5.25	6.11	4.97	5.69	4.73	5.21	4.82	5.05	5.35	6.38	4.62	6.02	4.65
Zr/Y	10.60	5.91	4.35	6.99	3.27	8.76	5.66	7.94	6.70	4.24	8.62	7.01	4.10	4.96	5.13
Cr/Ti	0.012	0.010	0.008	0.013	0.022	0.010	0.026	0.021	0.031	0.011	0.017	0.014	0.012	0.025	0.024
Cr/Th	15.53	15.08	11.74	10.67	6.01	14.04	12.18	12.14	11.71	9.34	13.98	10.65	10.98	14.35	5.52
La/Y	2.35	1.22	0.93	1.31	1.50	1.80	1.20	1.49	1.38	1.00	1.91	1.52	1.29	1.15	2.52
Th/Sc	0.73	1.21	2.06	2.61	0.84	2.09	0.90	2.06	2.93	1.51	2.09	2.56	3.59	0.84	0.76

Table 4. The contents of rare-earth elements ( $\mu\text{g/g}$ ) in the meta-argillo-arenaceous rocks

Number	1	2	3	4	5	6	7	8	9	10	11	12	13	14	15
Sample No.	Y5	Y61	Y65	Y8	X88	N1-3	Y60	X97	Y62	X14	X45	X50	X01	X37	X47
La	44.2	26.0	31.1	27.4	31.6	34.9	40.5	32.1	57.6	43.4	39.0	29.2	51.3	40.1	35.9
Ce	86.7	52.9	64.9	54.2	69.2	68.1	81.1	69.1	117	91.0	81.4	61.5	108	84.8	74.6
Pr	10.3	6.02	7.53	6.38	7.50	8.10	8.96	7.36	13.5	11.3	9.30	7.11	12.7	10.2	8.64
Nd	38.9	23.3	29.1	24.1	26.0	30.6	33.6	29.3	54.3	43.7	34.6	27.1	47.3	37.4	32.2
Sm	7.76	4.57	5.83	4.58	6.47	5.82	5.90	6.26	11.4	8.95	6.56	6.11	9.50	7.72	6.69
Eu	1.79	1.15	1.32	1.06	1.13	1.11	1.34	1.13	1.85	2.01	1.32	1.47	1.87	1.40	1.19
Gd	6.44	4.21	5.76	3.89	5.19	4.86	6.11	6.02	10.6	7.56	5.52	5.26	7.92	6.58	5.72
Tb	0.92	0.65	0.93	0.55	0.90	0.68	0.97	1.17	1.79	1.05	0.88	0.80	1.21	1.04	0.83
Dy	4.92	4.08	5.40	3.13	4.50	3.76	5.45	8.24	10.4	5.53	5.22	4.72	6.57	5.93	4.46
Ho	0.87	0.78	1.04	0.61	1.01	0.69	1.14	1.81	2.27	0.95	1.05	0.88	1.19	1.13	0.84
Er	2.43	2.22	2.70	1.68	3.05	2.11	2.91	5.35	6.20	2.43	2.95	2.54	3.40	3.39	2.40
Tm	0.36	0.32	0.41	0.26	0.37	0.33	0.47	0.80	0.97	0.35	0.48	0.41	0.48	0.51	0.33
Yb	2.32	2.14	2.58	1.81	2.23	2.31	2.74	5.50	6.76	2.35	3.08	2.81	3.32	3.53	2.28
Lu	0.34	0.31	0.35	0.27	0.32	0.36	0.39	0.77	0.94	0.37	0.46	0.41	0.50	0.54	0.34
TREE	208	129	159	130	159	164	192	175	296	221	192	150	255	204	176
LREE	190	114	140	118	142	149	171	145	256	200	172	133	230	182	159
HREE	18.6	14.7	19.2	12.2	17.6	15.1	20.2	29.7	39.9	20.6	19.6	17.8	24.6	22.7	17.2
L/H	10.2	7.75	7.29	9.65	8.08	9.84	8.49	4.90	6.40	9.73	8.77	7.43	9.38	8.02	9.26
La/Yb	19.0	12.2	12.1	15.2	14.2	15.1	14.8	5.84	8.52	18.5	12.7	10.4	15.4	11.3	15.8
$\delta\text{Eu}$	0.75	0.79	0.69	0.75	0.58	0.62	0.68	0.55	0.51	0.73	0.66	0.78	0.64	0.59	0.58
$\delta\text{Ce}$	0.93	0.96	0.97	0.93	1.03	0.92	0.96	1.02	0.96	0.95	0.98	0.98	0.97	0.97	0.97
La/Yb*	12.9	8.23	8.15	10.2	9.56	10.2	10.0	3.95	5.76	12.5	8.56	7.03	10.4	7.66	10.7

Table 4. (to be continued)

Number	16	17	18	19	20	21	22	23	24	25	26	27	28	29	30
Sample No.	X52	X67	X566	X30	X61	Y9	X62	X11a	X11d	X51	G2	G3	G4	Zk320	Zk47
La	39.2	30.2	27.2	35.5	34.9	45.1	32.0	36.1	41.0	40.4	51.4	42.6	38.7	45.9	43.1
Ce	74.9	62.5	53.5	76.6	70.1	92.2	65.3	75.8	85.0	83.3	106	90.2	80.8	96.5	93.7
Pr	8.21	7.31	7.16	7.43	8.37	9.61	7.73	8.86	9.85	9.51	12.5	10.30	10.1	11.0	10.8
Nd	30.7	28.2	27.4	34.1	32.7	33.0	30.2	32.8	35.9	35.3	46.7	39.4	36.8	41.2	41.3
Sm	6.05	5.44	5.71	6.94	6.86	7.81	6.29	6.31	7.06	7.83	9.31	7.42	7.80	8.51	9.20
Eu	1.24	1.48	1.25	1.41	1.35	1.45	1.38	1.21	1.37	2.06	1.62	1.37	1.48	2.02	1.80
Gd	4.84	4.91	5.30	6.29	5.98	6.14	5.86	5.67	5.98	7.06	7.58	6.40	7.16	7.92	7.80
Tb	0.64	0.74	0.89	1.03	1.13	1.06	0.97	0.84	0.89	1.10	1.06	0.98	1.29	1.22	1.30
Dy	3.54	4.51	5.62	4.90	6.04	4.86	5.68	4.95	5.58	6.58	5.70	5.44	6.40	7.32	8.00
Ho	0.68	0.95	1.09	1.01	0.95	1.17	1.09	0.93	1.11	1.36	1.04	1.04	1.36	1.44	1.70
Er	2.03	2.70	3.28	2.72	2.60	3.44	3.06	2.77	3.28	4.20	2.86	3.08	3.91	4.15	4.70
Tm	0.33	0.45	0.49	0.40	0.45	0.48	0.42	0.40	0.49	0.71	0.44	0.49	0.59	0.61	0.70
Yb	2.24	3.13	3.26	2.45	2.81	3.06	2.94	2.86	3.47	5.24	3.24	3.27	3.78	4.19	4.30
Lu	0.37	0.45	0.48	0.30	0.41	0.49	0.43	0.42	0.52	0.80	0.50	0.50	0.58	0.60	0.68
TREE	175	153	143	181	175	210	163	180	202	205	250	212	201	233	229
LREE	160	135	122	162	154	189	143	161	180	178	228	191	176	205	200
HREE	14.7	17.8	20.4	19.1	20.4	20.7	20.5	18.8	21.3	27.1	22.4	21.2	25.1	27.5	29.2
L/H	10.9	7.57	5.99	8.48	7.57	9.13	6.99	8.54	8.45	6.60	10.20	9.03	7.01	7.47	6.85
La/Yb	17.5	9.66	8.34	14.50	12.4	14.7	10.9	12.6	11.8	7.71	15.9	13.0	10.2	11.0	10.0
$\delta$ Eu	0.68	0.86	0.69	0.64	0.63	0.62	0.69	0.61	0.63	0.83	0.57	0.60	0.60	0.74	0.63
$\delta$ Ce	0.94	0.96	0.89	1.06	0.94	1.00	0.95	0.97	0.97	0.97	0.96	0.99	0.94	0.98	1.00
La/Yb*	11.8	6.52	5.64	9.80	8.40	9.95	7.36	8.52	7.99	5.21	10.7	8.81	6.92	7.41	6.77

Note: For sample Nos. and lithological characters, see Table 1; La/Yb\* is the chondrite-normalized ratio; La/Yb is the measured ratio of element contents.

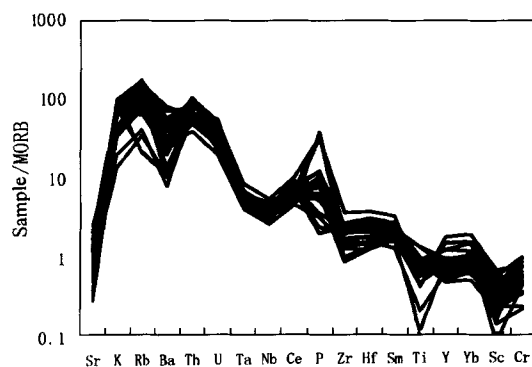


Fig. 4. A spider diagram of trace elements in the meta-argillo-arenaceous rocks.

#### 4.2 Rb-Sr isochron ages and Sm-Nd compositions of the meta-argillo-arenaceous rocks

On the basis of detailed research on the petrology (Hu Gongren et al., 1999b; Hu Gongren and Liu Congqiang, 2002; Hu Gongren et al., 2004) and geochemistry of major, REE and trace elements, Rb/Sr ratios in biotite minerals from the meta-argillo-arenaceous rocks were determined. Their Rb-Sr isotopic compositions were analyzed. Meanwhile the Rb-Sr compositions of amphibolites in the profile were also analyzed (Hu Gongren et al., 1997).

The Rb-Sr isotopic compositions of the meta-argillo-arenaceous rocks and their mineral compositions listed in Table 5 constitute an isochron with a calculated age of  $719.7 \pm 0.1$  Ma by using York's method [Fig.

5(a), York, 1969] with a high coefficient of correlation (0.9999) and small errors involved in age and initial  $^{87}\text{Sr}/^{86}\text{Sr}$  ratio. These suggest that the Sr isotopic system was homogenized in the whole rock on a profile scale during amphibolite metamorphism. The isochron age represents the time of metamorphism. The Rb-Sr isochron age ( $674 \pm 24$  Ma) of the metamorphic rocks at Qiwan, as well as in Zhuji (Shui Tao et al., 1988), is close to the time of metamorphism in this area.

The Sm-Nd isotopic compositions of samples from the meta-argillo-arenaceous rocks in the metamorphic belt of central Jiangxi Province are listed in Table 6. The sedimentation age assumed in the calculation of  $\epsilon_{\text{Nd}}$  values is 1113 Ma, based on the available Sm-Nd isochron age of  $1113 \pm 49$  Ma ( $\epsilon_{\text{Nd}}(t) = 2.4 \pm 0.1$ ,  $\text{MSWD} = 0.215$ ,  $r = 0.99827$ ) of plagioclase-amphibolite provided by Hu Gongren et al. (1999a). The Sm-Nd isotopic compositions of the samples only show slight variation [ $^{147}\text{Sm}/^{144}\text{Nd} = 0.10461 - 0.13252$ ,  $^{143}\text{Nd}/^{144}\text{Nd} = 0.511827 - 0.512052$ ,  $\epsilon_{\text{Nd}}(0) = -11.4 - -15.8$ ,  $\epsilon_{\text{Nd}}(1113) = 1.11 - -3.60$ ]. These data are similar to the Sm-Nd isotopic compositions of the Mayuan Group granulite in northern Fujian Province [ $^{147}\text{Sm}/^{144}\text{Nd} = 0.1145 - 0.1167$ ,  $^{143}\text{Nd}/^{144}\text{Nd} = 0.511970 - 0.511918$ ,  $\epsilon_{\text{Nd}}(0) = -12.8 - -13.0$ ,  $\epsilon_{\text{Nd}}(1129) = -1.15 - -1.25$ ,  $t_{\text{DM}} = 1810 - 1835$  Ma] provided by Chen Diyun (1994). In  $\epsilon_{\text{Nd}}(t)$ - $t$  diagram (Fig. 5b), they have similar evolution fields and trends, indicating they have similar material



sources. They are obviously different from the Sm-Nd isotopic signatures [ $\epsilon_{Nd}(0) = -8.27 - -9.44$ ,  $t_{DM} = 1522 - 1699$  Ma] of Presinian metasediments in north-

eastern Jiangxi and southern Anhui provinces (Chen Jianfen, 1989).

**Table 5. Rb-Sr isotopic compositions of the meta-argillo-arenaceous rocks of the metamorphic belt in central Jiangxi Province**

Sequence No.	Sample No.	Rock type or mineral	Rb ( $\mu\text{g/g}$ )	Sr ( $\mu\text{g/g}$ )	$^{87}\text{Rb}/^{86}\text{Sr}$	$^{87}\text{Sr}/^{86}\text{Sr}$	2 $\sigma$	Calculated result
1	X14	Biotite	361.9	17.19	60.03	1.333112	28	$t = 719.7 \pm 0.1$ Ma
2	X45	Biotite	352.8	16.89	59.54	1.328317	25	$I_r = 0.71662 \pm 0.00006$
3	X47	Whole rock	90.67	35.49	7.383	0.792429	30	$r = 0.99993$
4	X50	Whole rock	123.6	153.4	2.302	0.740243	20	
5	X67	Whole rock	80.12	299.6	0.7625	0.724486	18	
6	X566	Whole rock	19.07	66.36	0.3690	0.719026	14	

**Table 6. Sm-Nd isotopic compositions and calculated parameters for the meta-argillo-arenaceous rocks of the metamorphic belt in central Jiangxi Province**

Sample No.	Sm	Nd	$^{147}\text{Sm}/^{144}\text{Nd}$	$^{143}\text{Nd}/^{144}\text{Nd}$	2 $\sigma$	$f_{\text{Sm}/\text{Nd}}$	$t_{\text{CHUR}}$	$t_{\text{DM}}$	$\epsilon_{\text{Nd}}(1113)$	$\epsilon_{\text{Nd}}(0)$	Th/Sc
X45	7.135	35.67	0.12100	0.511901	25	-0.39	1481	2050	-3.60	-14.4	2.134
X50	3.352	17.28	0.11731	0.512045	16	-0.40	1138	1746	-0.25	-11.6	1.564
X47	5.265	24.03	0.13252	0.512017	28	-0.33	1472	2124	-2.98	-12.1	1.773
G4	7.890	42.58	0.10461	0.511827	18	-0.47	1341	1846	-2.70	-15.8	3.599
X67	5.350	27.74	0.10871	0.512052	22	-0.45	1015	1597	1.11	-11.4	1.212
Y8	19.64	94.95	0.11670	0.512038	16	-0.41	1142	1746	-0.30	-11.7	1.200
Y5	4.590	24.32	0.11417	0.511876	14	-0.42	1405	1948	-3.11	-14.9	0.913

Note: 1.  $t_{\text{DM}}$  and calculated age from  $\epsilon_{\text{Nd}}$  value in Ma;  $t_{\text{CHUR}} = (1/\lambda) \ln \{ [ (^{143}\text{Nd}/^{144}\text{Nd}) - 0.512638 ] / [ (^{147}\text{Sm}/^{144}\text{Nd}) - 0.1967 ] + 1 \}$ ; 2. the equation for calculating model ages;  $t_{\text{DM}} = (1/\lambda) \ln \{ [ (^{143}\text{Nd}/^{144}\text{Nd}) - 0.51315 ] / [ (^{147}\text{Sm}/^{144}\text{Nd}) - 0.2136 ] + 1 \}$ ;  $\lambda = 6.54 \times 10^{-12} \text{ a}^{-1}$ .

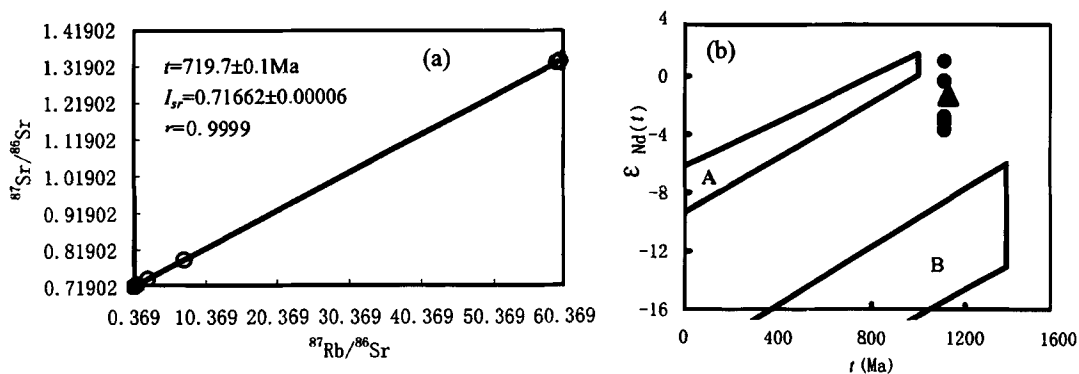


Fig. 5. (a) Rb-Sr isochron diagram of the meta-argillo-arenaceous rocks of the metamorphic belt in central Jiangxi Province. (b)  $\epsilon_{\text{Nd}}(t)$ - $t$  evolutionary diagram of meta-argillo-arenaceous rocks of the metamorphic rock belt in central Jiangxi Province and its neighboring areas. ● Meta-argillo-arenaceous rocks of the metamorphic rock belt in central Jiangxi Province; ▲ metasediments of the Mayuan Group in northern Fujian Province. A. Pre-Sinian metasediments in northeastern Jiangxi and southern Anhui provinces (Chen Jianfen et al., 1989); B. metasediments of the Chencai Group in Longquan and eastern Zhejiang (Xu Butai et al., 1989).

In the  $\epsilon_{\text{Nd}}(t)$ - $t$  evolution diagram, the data of all the samples from the meta-argillo-arenaceous rocks of the metamorphic belt in central Jiangxi Province and the Mayuan Group granulite in northern Fujian Province are plotted out of the field of Presinian metasediments in northeastern Jiangxi and southern Anhui provinces (Xu Butai, 1989). Therefore, their rock-forming detritus could not possibly come from the Yangtze

Block in the north, but should come from Archean rocks in the northeast, as granulite and plagiogneiss of the Archean Chencai Group have an old  $t_{\text{DM}}$  of 2350 - 2832 Ma, and low values of  $\epsilon_{\text{Nd}}(0) = -19.66 - -26.59$  as indicated by Xu Butai (1989).

## 5 Discussion

### 5.1 The forming age of the metamorphic belt in central Jiangxi Province

The Nd isotopic compositions of argillo-arenaceous rocks not only reflected the position of source areas, but also played an important role in determining the forming age of the argillo-arenaceous rocks. It is believed that the metamorphic belt in central Jiangxi Province underwent complicated metamorphism and deformation more than once, as their  $t_{DM}$  values vary from 1597 Ma to 2124 Ma, though there is no obvious transformation of REE in the rocks. All the analyzed samples are fresh, with no intense affect of exogenetic weathering. Meta-argillo-arenaceous rocks in the metamorphic belt in central Jiangxi Province are higher in maturity. They were sediments derived from intra-recycling processes. On the basis of the definition of Sm-Nd isotope depleted mantle age,  $t_{DM}$  of 1597 – 2124 Ma should reflect the formation age of source rocks, not represent the formation age of the metamorphic belt in central Jiangxi Province, only providing the maximum deposition age of the original sedimentary rocks in central Jiangxi Province. According to the whole-rock Sm-Nd isochron ages ( $1113 \pm 49$  Ma to  $1199 \pm 26$  Ma) (Den Guohui, 1997; Hu Gongren et al., 1999a; Yu Dagan et al., 1999) of plagioclase-amphibole (schist) and Nd isotopic model age  $t_{DM}$  (1597 – 2124 Ma) of meta-argillo-arenaceous rocks, the metamorphic rock belt in central Jiangxi Province was formed during the Middle Proterozoic between 1100 – 1600 Ma.

### 5.2 Source-rock weathering characteristics

Th/U ratios in most rocks are typically between 3.5 and 4.0 (McLennan et al., 1993). The Th/U ratios of all samples (3.40 – 6.42, only one lower than 3.8) are generally higher than 3.8 (Archean upper crust). The Th/U ratios which are higher than 4.0

may indicate that the source rocks were intensively weathered, sedimentarily recycled (i. e., derivation from older sedimentary rocks) or derived mainly from felsic igneous rocks (Fedo et al., 1996). The Th/U versus Th plot for samples (Fig. 6a) shows a typical distribution similar to that of the average values of fine-grained sedimentary rocks reported by Taylor and McLennan (1985) with a normal weathering trend (McLennan et al., 1993). Therefore, it is believed that the sources of meta-argillo-arenaceous rocks were recycled sediments and/or might have undergone intensive weathering.

Sedimentary sorting and recycling can be monitored by a plot of Th/Sc against Zr/Sc, as indicated by McLennan et al. (1993). First-order sediments show a simple positive correlation between the two ratios, whereas recycled sediments show a substantial increase in Zr/Sc with a far less increase in Th/Sc. On the Th/Sc versus Zr/Sc diagram, meta-argillo-arenaceous rocks follow a general trend consistent with their direct derivation from igneous rocks (Fig. 6b). It can be, therefore, inferred from Figs. 6(a) and (b) that the bulk of meta-argillo-arenaceous rocks was directly derived from igneous rocks that had undergone more intensive weathering.

Studies of modern weathering showed that Ca, Na and Sr are rapidly lost during chemical weathering and that the loss amount of these elements is proportional to the degree of weathering (Wronkiewicz and Condie, 1989). Two major-element indices [CIA (chemical index of alteration) and CIW (chemical index of weathering); Nesbitt and Young, 1982; Harnois, 1988] were proposed to monitor chemical weathering, only the CIW index avoids problems related to the remobilization of K during diagenesis or metamorphism. Unweathered UC (upper crust) generally has CIW indices between 55 and 60 and average Sr contents of

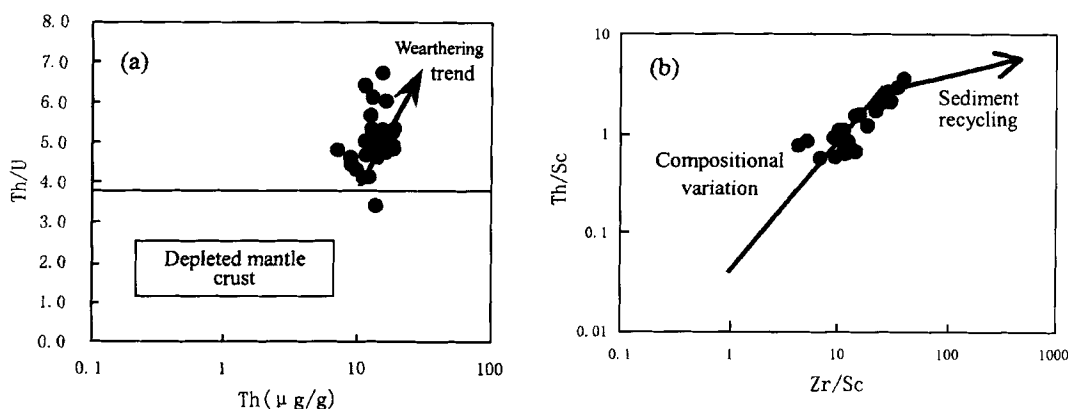


Fig. 6. Plots of (a) Th/U versus Th and (b) Th/Sc versus Zr/Sc for the meta-argillo-arenaceous rocks (Crichton and Condie, 1993).

250 – 300  $\mu\text{g/g}$ . In the CIW-Sr diagram (diagrams omitted), only 5 samples with CIW indices of 53.17 – 66.68, 25 samples with CIW indices of 69.30 – 95.94, 19 samples with CIW indices of  $>79$ , 24 samples with CIA indices of 60.5 – 76.8 (average value close to that of the average shale (70 – 75), and Sr contents of 50 – 250  $\mu\text{g/g}$ . All this suggests that the weathering degree of the source rocks is probably very intense and the source rocks are very mature.

The Al-Ti-Zr ternary diagram reflects the effects of sorting processes (Garcia et al., 1994). On this diagram, mature sediments consisting of both sandstones and shales show a wide range of  $\text{TiO}_2/\text{Zr}$  variations. On the Al-Ti-Zr diagram (diagrams omitted), samples show a wide range of  $\text{TiO}_2/\text{Zr}$  variations, indicating intense sorting and slow deposition of the sediments.

### 5.3 Composition of source rocks

Generally, REE, HFSE (high field strength elements), Th, Sc, Hf and Co can reflect the composition of source rocks (Condie and Wronkiewicz, 1990b). On the MORB-normalized spider diagram (Fig. 4), samples are characterized by strong enrichment in K, Rb, Ba, Th, U, Ta, Nb, Ce and P,

slight enrichment in Zr, Hf, Sm, Y and Yb, and strong depletion in Ti and Sc. These characteristics indicate that the samples were derived from granite source (Condie, 1993). Lower Sr contents are related to intense chemical weathering, higher incompatible element contents indicate that the source region is more differential (Camire et al., 1993).

A plot of La/Th vs. Hf (Fig. 7a) provides a useful tool for bulk rock discrimination between different arc compositions and sources (Floyd and Leveridge, 1987). Felsic composition-dominated arcs have low and uniform La/Th ratios ( $< 5$ ) and Hf contents of about 3 – 7  $\mu\text{g/g}$ . With the progressive unroofing of the arc and/or incorporation of sedimentary basement rocks, the Hf content increases via the release of zircon (Floyd and Leveridge, 1987). The compositions of meta-argillo-arenaceous rocks from the metamorphic rock belt in central Jiangxi Province suggest that they were originally derived from acidic arc sources with minor old sediment component (Fig. 7a). In the  $\epsilon_{\text{Nd}}(0)$ -Th/Sc diagram, samples are plotted close to the field of UC (Fig. 7b), indicating the composition of source rocks is similar to that of the modern upper crust.

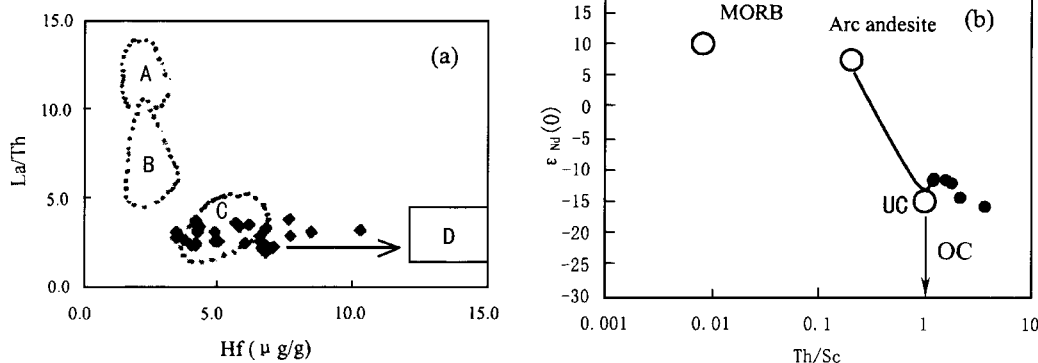


Fig. 7. Plots of (a) La/Th versus Hf (Fedo et al., 1996) and (b)  $\epsilon_{\text{Nd}}(0)$ -Th/Sc (McLennan et al., 1990) for meta-argillo-arenaceous rocks. UC. Upper crust; OC. old crust. A. Tholeiitic oceanic island arc source; B. andesitic arc source; C. acidic arc source; D. passive margin source.

In the Cr/Ti-Zr/Y diagram (diagrams omitted) (Crichton and Condie, 1993), Cr/Ti ratios (0.01 – 0.052) of 27 samples are obviously higher than those of the Witwatersrand Supergroup and Pongloar Supergroup in South Africa, slightly higher than the average value (0.012) of Archean granite and TTG, and lower than the average value (0.07) of Archean basalts. All these reflect that sediments were derived mainly from granite source.

Cr/Th ratios in Pelite are controlled most strongly

by the effects of local provenance and local tectonics. It is a sensitive indicator of provenance and can record variations in composition of the upper crust (Condie and Wronkiewicz, 1990a). Cr/Th ratios (3.31 – 14.25) of samples are obviously lower than the average value (31) of the Archean upper crust (Condie and Wronkiewicz, 1990a). This reflects preferential enrichment of granite, short of komatiite and basalt for source rocks.

The strongly incompatible element Th and the com-

patible element Sc are both quantitatively depositional continental sedimentary during sedimentation. Th/Sc ratios show a greater sensitivity for distinguishing the source rocks, and reflect the relative granite/(komatiite + basalt) ratio of the source rocks. Th/Sc ratios (1.00–3.60) of samples are obviously higher than those of apogite of the Archean greenstone belt ( $<1$ ), Archean sedimentary rocks ( $<1$ ) and typical Archean craton sediments (e. g. the Witwatersrand Supergroup and Pongloar Supergroup). These indicate that the rocks were formed in a stable crust tectonic setting. In the La-Th-Sc diagram (diagrams omitted; Wronkiewicz and Condie, 1989), the data for the samples are generally distributed along a mixing parallel line defined by granite and basalt, and are plotted into the granite field. This indicates the original sedimentary rocks were mainly derived from granite components.

The Ni and Cr contents of sedimentary rocks indicate the contribution to mafic-ultramafic rock sources. Ni (20.1–72.1  $\mu\text{g/g}$ ) and Cr (45.7–209  $\mu\text{g/g}$ ) contents of samples are lower than those of the Archean sedimentary rocks (Condie and Wronkiewicz, 1990b). In the Ni-Cr diagram (diagrams omitted), the data for the samples are mainly plotted into the straddle of the Post-Archean and Neo-Archean shales, Ni and Cr contents slightly lower than those of the Beit

Bridge Group (metamorphic continental rift), Witwatersrand Supergroup and Pongloar Supergroup (typical craton sediments) in South Africa. Low Ni and Cr contents indicate lower mafic components in the source rocks. Contributions of komatiite/granite sources should be reflected by the distribution of Cr/Zr ratios, since these two elements monitor chromite and zircon contents, respectively (Wronkiewicz and Condie, 1989). Cr/Zr ratios (0.26–1.14) of the samples are obviously lower than those of shales of the Witwatersrand Supergroup and pelite of the Pongloar Supergroup in South Africa. This indicates that sediments were mainly sourced from acidic arc rocks.

In the  $\delta\text{Eu}-(\text{Gd}/\text{Yb})_N$  diagram (diagrams omitted), the data for the samples are characterized by moderate negative Eu anomalies, and are plotted into the post-Archean sedimentary rock fields. Compared to PAAS, the samples are characterized by higher LREE enrichment, flat heavy REE patterns and relatively less fractionated light rare earth patterns [ $(\text{La}/\text{Eu})_N = 4.48 - 7.28$ ,  $(\text{La}/\text{Yb})_N = 3.95 - 12.9$ ]. As mentioned above, their source materials are composed dominantly of upper crust source rocks (Al- and K-rich granitic or/and sedimentary rocks of Early Proterozoic) (Chen et al., 1990).

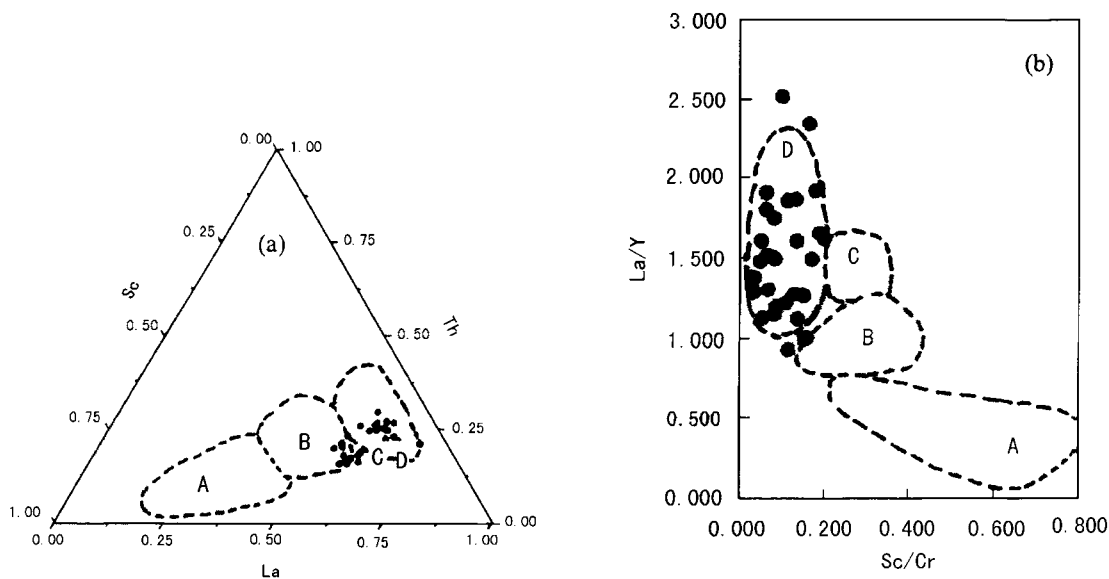


Fig. 8. Plots of (a) La-Sc-Th and (b) La/Y-Sc/Cr for meta-argillo-arenaceous rocks (Bhatia and Crook, 1986). A. Oceanic island arc; B. continental island arc; C. active continental margin; D. passive continental margin.

#### 5.4 Tectonic environment

Compared to the REE and trace element parameters for sedimentary rocks in various tectonic settings

(Bhatia and Crook, 1986), the meta-argillo-arenaceous rocks from the metamorphic belt in central Jiangxi Province have relatively high contents of LREE [i. e.,  $(\text{La}/\text{Sm})_N = 2.86 - 4.19$ ],  $\Sigma\text{REE} = 129 -$

296  $\mu\text{g/g}$ , moderate negative Eu anomalies ( $\delta\text{Eu} = 0.51 - 0.86$ ),  $(\text{La}/\text{Yb})_N = 3.95 - 12.9$ ,  $\text{Th}/\text{Sc} = 0.57 - 3.59$ ,  $\text{La}/\text{Sc} = 1.46 - 12.4$ ,  $\text{La}/\text{Yb} = 5.84 - 19.0$ , high Th/U ratios (3.60 - 6.42), and low La/Th values (2.00 - 3.78). These indicate that the original sediments were deposited in the continental margin tectonic environment (Bhatia and Crook, 1986). In the La-Th-Sc discrimination diagram (Fig. 8a), the data for the samples are mainly plotted into the fields of continental margins (C + D) and the continental island arc. The variation of La/Y against Sc/Cr is displayed in Fig. 8b. Most samples are plotted into the field of passive continental margins (D).

In the  $\lg(\text{Na}_2\text{O}/\text{K}_2\text{O}) - \lg(\text{SiO}_2/\text{Al}_2\text{O}_3)$  diagram (diagrams omitted; Pettijohn, 1975), the source-area rocks consist mainly of feldspathic sandstones, minor greywacke and fragmental sandstones. This reflects they were probably formed by slow deposition in an inactive tectonic environment. The REE distribution patterns, LREE contents, and  $(\text{La}/\text{Sm})_N$ ,  $(\text{La}/\text{Yb})_N$ ,  $\text{Eu}/\text{Eu}^*$  ratios of our samples are similar to those of PAAS. This reflects they were deposited in a passive margin tectonic environment as suggested by McLennan (1989).

The fairly homogeneous Nd isotopic compositions indicate that the sediments were derived from the same source. Various sedimentary components were completely mixed during pre-deposition. In the  $\varepsilon_{\text{Nd}}(0) - \text{Th}/\text{Sc}$  diagram, the relationship between  $\varepsilon_{\text{Nd}}(0)$  and Th/Sc indicates that the original rocks of meta-argillo-arenaceous rocks from the metamorphic belt in central Jiangxi Province were deposited at the trailing edges of a passive margin tectonic environment (McLennan et al., 1990, 1991).

## 6 Geological significance

Geochemical evidence shows that meta-argillo-arenaceous rocks from the metamorphic belt in central Jiangxi Province originally represent a suit of cratonic sedimentary rocks. These rocks are characterized by high LREE and LILE contents, moderate negative Eu anomalies ( $\delta\text{Eu} = 0.51 - 0.86$ ), flat heavy REE patterns [ $(\text{La}/\text{Eu})_N = 4.48 - 7.28$ ,  $(\text{La}/\text{Yb})_N = 3.95 - 12.9$ ],  $\text{Th}/\text{Sc} = 0.57 - 3.59$ ,  $\text{La}/\text{Sc} = 1.46 - 12.4$ ,  $\text{La}/\text{Yb} = 5.84 - 19.0$  and higher Th/U ratios (3.60 - 6.42), lower La/Th values (2.00 - 3.78), and relatively low Zr, Hf, Sc, Ti, HREE and Sr contents. They have similar lithologic characters, metamorphic grade (Deng Jiarui and Zhang Zhiping, 1998) and Sm-Nd isotopic compositions to those of rocks of the Mayuan Group in northern Fujian Province, with

similar evolution fields and trends as seen in the  $\varepsilon_{\text{Nd}}(t) - t$  diagram. This indicates that they have similar original material sources and the same deposition environment of the cratonic continental raft shallow-sea. The original rocks should be a suit of shallow-facies argillo-arenaceous flysch formations. Their source materials were composed dominantly of upper crust-source rocks (Al- and K-rich granitic or/and sedimentary rocks of Early Proterozoic). Eastern Cathaysian block underwent intracrustal differentiation during the Neo-Archean and Early Proterozoic, and source materials/rocks experienced strong chemical weathering. They are the most important signs of exogenetic process of Cathaysian block cratonization during the Proterozoic.

**Acknowledgements** The authors wish to thank Geological Party No. 261, East China Bureau of Geology, China National Nuclear Corporation for their help with field work, Institute of Geochemistry, Chinese Academy of Sciences for ICP-MS analyses, State Key Laboratory for Mineral Deposits Research, Nanjing University for major element oxides analyses, Laboratory of Isotope Mass Spectrometry under the Modern Analytical Center of Nanjing University for Rb-Sr isotope analyses, and Radiogenic Isotope Laboratory at Beijing Research Institute of Uranium Geology for Sm-Nd isotope analyses.

## References

- Bhatia M. R. and Crook K. A. W. (1986) Trace element characteristics of graywackes and tectonic setting discrimination of sedimentary basins [J]. *Contrib. Mineral Petrol.* **92**, 181 - 193.
- Camire G. E., Lafleche M. R., and Ludden N. J. (1993) Archean metasedimentary rocks from the northwestern Pontiac subprovince of the Canadian shield: Chemical characterization, weathering and modeling of the source areas [J]. *Precambrian Research.* **62**, 285 - 305.
- Chen C. H., Jhan B. M., Lee T. et al. (1990) Sm-Nd isotopic geochemistry of sediments from Taiwan and implications for the tectonic evolution of Southeast China [J]. *Chem. Geol.* **88**, 317 - 332.
- Chen Diyun (1994) *The Source of Ore-Forming Materials and Genesis Study of Volcanic U (Ag, Mo) Deposits in North Wuyi Mountains* [D]. Nanjing, Nanjing University (in Chinese).
- Chen Jianfen (1989) The sediment source and Nd isotopic composition of low-grade metamorphic rocks and sediments from South Anhui [J]. *Bulletin of Science.* **20**, 1572 - 1574 (in Chinese with English abstract).
- Condie K. C. (1993) Chemical composition and evolution of the upper continental crust: Contrasting results from surface samples and shales [J]. *Chemical Geology.* **104**, 1 - 37.
- Condie K. C. and Wronkiewicz D. J. (1990a) Evolution of the Kaapvaal craton: The Cr/Th ratio in pelites as an index of craton maturation [J]. *Earth Planet Science Letter.* **97**, 256 - 267.
- Condie K. C. and Wronkiewicz D. J. (1990b) A new look at the Archean-Proterozoic boundary sediments and the tectonic setting constraint. In *Precambrian Continental Crust and Its Economic Resources* [C] (ed. Naqvi S. M.). pp. 61 - 83. Elsevier, Amsterdam.

- Condie K. C., Boryta M. D., Liu Jinzhong et al. (1992) The origin of khondalites: Geochemical evidence from the Archean to early Proterozoic granulite belt in the North China craton [J]. *Precambrian Research*. **59**, 207 – 223.
- Crichton J. G. and Condie K. C. (1993) Trace elements as source indicators in cratonic sediments: A case study from the Early Proterozoic Libby Creek Group, southeastern Wyoming [J]. *Journal of Geology*. **101**, 319 – 332.
- Den Guohui (1997) Characteristics of amphibolite in Yaoxu, Dongxiang-Maquan, Yujiang region and its significance [J]. *Geological Science and Technology of Jiangxi*. **24**, 20 – 24 (in Chinese with English abstract).
- Deng Jiarui and Zhang Zhiping (1998) Late Precambrian tectonic framework in Fujian, Zhejiang and Jiangxi [J]. *Geological Review*. **44**, 561 – 566 (in Chinese with English abstract).
- Fedo C. M., Eriksson A. K., and Krogstad E. (1996) Geochemistry of shales from the Archean (~3.0 Ga) Buhwa greenstone belt, Zimbabwe: Implications for provenance and source-area weathering [J]. *Geochimica et Cosmochimica Acta*. **60**, 1751 – 1763.
- Floyd P. A. and Leveridge B. E. (1987) Tectonic environment of the Devonian mode and geochemical evidence from turbiditic sandstones [J]. *J. Geol. Soc.* **144**, 531 – 542.
- Garcia D., Fonteilles M., and Moutte J. (1994) Sedimentary fractionations between Al, Ti, and Zr and the genesis of strongly peraluminous granites [J]. *J. Geol.* **102**, 411 – 412.
- Gibbs A. K., Montgomery C. W., O-Day P. A. et al. (1986) The Archean-Proterozoic transition: Evidence from the geochemistry of metasedimentary rocks of Guyana and Montana [J]. *Geochim. Cosmochimica Acta*. **50**, 2125 – 2141.
- Gromet L. P., Dymek R. F., Haskin L. A. et al. (1984) The "North American Shale Composite": Its compilation major and trace element characteristics [J]. *Geochim. Cosmochimical Acta*. **48**, 2469 – 2482.
- Harnois L. (1988) The CIW index: A new chemical index of weathering [J]. *Sed. Geology*. **55**, 319 – 322.
- He Gaopin (1986) The research method for the original rocks of metamorphic rocks [J]. *J. Changchun Geol. Univ.* **4**, 31 – 35 (in Chinese with English abstract).
- Hu Gongren and Liu Congqiang (2002) Geochemistry of amphibolites from the Zhoutan Group, Jiangxi Province: Implications for the tectonic settings [J]. *Acta Mineralogica Sinica*. **22**, 335 – 342 (in Chinese with English abstract).
- Hu Gongren and Zhang Bangtong (1998a) Neodymium isotope composition and source materials of the meta-basement in central Jiangxi Province [J]. *Acta Petrologica et Mineralogica*. **17**, 35 – 39 (in Chinese with English abstract).
- Hu Gongren, Liu Congqiang, Zhang Bangtong et al. (2004) Geochemical characteristics of meta-argillo-arenaceous rocks from the metamorphic rock belt in central Jiangxi Province and its geological significance [J]. *Geochimica*. **33**, 118 – 130 (in Chinese with English abstract).
- Hu Gongren, Zhang Bangtong, and Wang Changhua (1997) First determination of the Neoproterozoic metamorphic rocks in Xiangshan, central Jiangxi Province [J]. *Regional Geology of China*. **16**, 222 – 224 (in Chinese with English abstract).
- Hu Gongren, Zhang Bangtong, and Wang Xiangyun (1998b) Mineralogy, petrology and isotopic geochemistry of the Proterozoic amphibolites from Xiangshan, central Jiangxi Province [J]. *Geochimica*. **27**, 217 – 229 (in Chinese with English abstract).
- Hu Gongren, Zhang Bangtong, and Yu Ruilian (1999a) A study on Sm-Nd and Rb-Sr isochron ages of the central Jiangxi metamorphic belt [J]. *Geological Review*. **45**, 129 – 134 (in Chinese with English abstract).
- Hu Gongren, Zhang Bangtong, and Yu Ruilian (1999b) Petrology, age and geochemistry of the Proterozoic amphibolites from Xiangshan, central Jiangxi Province [J]. *Chinese Journal of Geochemistry*. **18**, 139 – 149.
- Li Jieyuan (1992) The Sm-Nd isochron ages measuring of rocks and mineral [J]. *Bulletin of Nuclear Industry, Beijing Geological Academy*. **10**, 35 – 37 (in Chinese with English abstract).
- McLennan S. M. (1989) Rare-earth elements in sedimentary rocks: Influence of provenance and sedimentary processes [J]. *Mineral. Soc. Amer. Rev. Mineral.* **21**, 169 – 200.
- McLennan S. M. and Taylor S. R. (1991) Sedimentary rocks and crustal evolution: Tectonic setting and secular trends [J]. *Journal of Geology*. **99**, 1 – 21.
- McLennan S. M., Hemming S. R., and Taylor S. R. (1995) Early Proterozoic crustal evolution: Geochemical and Nd-Pb isotopic evidence from metasedimentary rocks, southwestern North America [J]. *Geochim. Cosmochim. Acta*. **59**, 1153 – 1177.
- McLennan S. M., Hemming S. R., McDaniel D. K. et al. (1993) Geochemical approaches to sedimentation, provenance and tectonics. In *Processes Controlling the Composition of Clastic Sediments* [C] (eds. Johnsson M. L. and Basu A.). *Geol. Soc. Amer. Spec. Paper*. **284**, 21 – 40.
- McLennan S. M., Taylor S. R., McCulloch M. T. et al. (1990) Geochemical and Nd-Sr isotopic composition of deep-sea turbidites: Crustal evolution and plate tectonic association [J]. *Geochimica Cosmochimica Acta*. **54**, 2015 – 2050.
- Naqvi S. M., Sawkar R. H., Subba R. D. V. et al. (1988) Geology, geochemistry and tectonic setting of Archean graywackes from Karnataka Nucleus, India [J]. *Precambrian Res.* **39**, 193 – 216.
- Nesbitt H. W. and Young G. M. (1982) Early Proterozoic climates and plate motions inferred from major element chemistry of lutites [J]. *Nature*. **299**, 715 – 717.
- Pettijohn E. J. (1975) *Sedimentary Rocks (3rd ed)* [M]. pp. 628. Harper & Row, Publishers Inc, New York.
- Reimer T. O., Condie K. C., and Georgi A. (1985) Petrography and geochemistry of granitoid and metamorphic pebbles from the Early Archean Moodies Group, Barberton Mountainland/South Africa [J]. *Precambrian Research*. **29**, 383 – 404.
- Shui Tao, Xu Butai, Ling Ruhua et al. (1988) *Metamorphic Basement Geology in Zhejiang and Fujian Province* [M]. pp. 140. Science Press, Beijing (in Chinese).
- Taylor S. R. and McLennan S. M. (1985) *The Continental Crust: Its Composition and Evolution* [M]. pp. 9 – 56. Blackwell, Oxford.
- Taylor S. R. and McLennan S. M. (1995) The geochemical evolution of the continental crust [J]. *Rev. Geophys.* **33**, 241 – 265.
- Wang Renmin, He Gaopin, Chen Zhengzheng et al. (1987) *The Distinguishing Diagram for the Original Rocks of Metamorphic Rocks* [M]. pp. 41 – 45. Geological Publishing House, Beijing (in Chinese).
- Winkler H. G. F. (1976) *The Genetic of Metamorphic Rocks* [M]. pp. 100 – 105. Science Press, Beijing.
- Wronkiewicz D. J. and Condie K. C. (1989) Geochemistry and provenance of sediments from the Pongola Supergroup, South Africa: Evidence for a 3.0-Ga-old continental craton [J]. *Geochimica et Cosmochimica Acta*. **53**, 1537 – 1549.
- Xu Butai (1989) A study on isotope, rare-earth element geochemistry and geological chronology of metamorphic rocks from volcanic region in the East of Zhejiang [J]. *Zhejiang Geology*. **5**, 52 – 58 (in Chinese with English abstract).
- York D. (1969) Least-squares fitting of a straight line with correlated errors [J]. *Earth Planet. Sci. Lett.* **5**, 320 – 324.
- Yu Dagan, Ai Guigen, Huang Guofu et al. (1999) Isotopic age features and their geological implication of the Zhoutan Group in Jiangxi [J]. *Acta Geoscientia Sinica*. **20**, 195 – 200 (in Chinese with English abstract).